



COB-2021-0813

STUDY OF THE DESTABILIZATION OF EMULSIONS BY SHEAR-INDUCED COALESCENCE

Patricia Almeida Tristão
Ricardo Hadlich Teixeira Leite
Eliana Paola Marín Castaño
Lara Schimith Berghe
Paulo Roberto de Souza Mendes

Mechanical Engineering department, Pontifícia Universidade do Rio de Janeiro
patricialmeida2998@gmail.com, rtleite@puc-rio.br, epmarinc1053@puc-rio.br, lara.schimith@gmail.com, pmendes@puc-rio.br

Erick Fabrizio Quintella Andrade Coelho

Petrobras
erick.quintella@petrobras.com.br

Abstract. *The co-production of water in oil wells is one of the most challenging aspects of the petroleum industry since these fluids emulsify during transport within the pipelines. Since W/O emulsions possess higher apparent viscosity, their presence causes an increase in transport and processing costs. This research aims to analyze the influence of droplet deformation on emulsion stability, specifically, to study the increase in phase separation due to coalescence generated by shear-induced deformation on droplets. Initially, we studied the efficiency of the phase separation under different shear rates and shear times on a Couette geometry. The formation of large droplets was macroscopically observed, and the increase in phase separation efficiency was verified. Afterward, we modified the flow geometry, introducing coalescence and sedimentation zones, notoriously optimizing the phase separation process. The effect of deformation on stability was observed in both studies since the phase separation of the emulsions that suffered deformation was significantly higher than of those which remained at rest.*

Keywords: *emulsion, phase separation, crude oil, shear-induced coalescence*

1. INTRODUCTION

Water-in-oil emulsions are formed during the production and transport of oil (Yang *et al.*, 2007; Fortuny *et al.*, 2007; Fan *et al.*, 2010; Spiecker and Kilpatrick, 2004). Water is dispersed as droplets in the continuous oil phase as droplets, which are stabilized by natural surfactants present in the crude oil (Dicharry *et al.*, 2006; Samaniuk *et al.*, 2015; Rane *et al.*, 2015; Zarkar *et al.*, 2015; Pauchard *et al.*, 2014). Water content is one of the factors considered in the benchmark of crude oil prices. Thus, it is crucial to destabilize these emulsions in oil processing plants. Among the primary separation processes, gravitational settlers should be highlighted. These are pressure vessels designed to allow the separation of free water from the mixture through droplet sedimentation (Aleem and Mellon, 2018, 2012). Coalescence also plays an important role on this process since increasing the average droplet size increases the sedimentation rate. However, smaller droplets usually remain in suspension and the emulsion is transferred to an electrostatic coalescer.

When an external electric field is applied to water-in-oil emulsions, droplets are polarized and stretched by the electrostatic field inducing a dipole (Aleem and Mellon, 2012; Kamp *et al.*, 2017). Oppositely charged dipoles attract each other, approach, come into contact, and finally coalesce into larger ones (He *et al.*, 2020). This approach between adjacent droplets is also favored by the deformation of droplets caused by the electric field. However, a high electric field increases the risk of droplet breakup (Allan and Mason, 1962; Eow and Ghadiri, 2003), which generates smaller droplets and increases of emulsification stability (Karyappa *et al.*, 2016; Li *et al.*, 2021). The deformation of droplets caused by flow has been widely studied (Leal, 2004; Fischer and Erni, 2007) in the last few decades. Both experimental (Korobko *et al.*, 2005; Chen *et al.*, 2009; Gouseti *et al.*, 2020; Mazumdar *et al.*, 2017; De Bruyn *et al.*, 2013) and numerical (Barai and Mandal, 2019; Vu, 2019) studies concluded that flow may increase coalescence rate by deforming droplets and bringing them close together. Flow-induced coalescence is especially efficient in confined spaces (De Bruyn *et al.*, 2013). Even though the increase in coalescence rate is likely to favor phase separation, to the best of our knowledge, there is no study correlating flow-induced coalescence to an increase in the phase separation process efficiency.

The objective of this work is to demonstrate that flow-induced coalescence leads to an optimization in the efficiency of the gravity separation process. In the present paper, we conduct an experimental analysis in a confined space apparatus

and compare the phase separation efficiency for various shear rates, shearing times, and flow geometries.

2. MATERIALS AND METHODS

The dispersed phase is synthetic water, based on ASTM D1141 - 98 technical standard. It constitutes 40% in volume fraction for each emulsion. Consequently, the continuous phase represents 60% of the total volume. Primol 352 from Exxon Mobil and Span 85 from Sigma-Aldrich are the materials that comprise this continuous phase. Table 1 shows the composition of the organic phase for the two systems used in the experiments, while Table 2 shows the interfacial tension between the organic phase and the aqueous phase for each of those systems.

Table 1. % weight of each material in the organic phase

	Oil 1	Oil 2	Oil 3
Primol 352 ($\rho = 0.851g/ml$)	99.76	99.69	99.55
Span 85 ($\rho = 0.956g/ml$)	0.24	0.30	0.45

Table 2. Interfacial tension between the organic phase and the aqueous phase for each system

	Interfacial Tension (N/m)
System 1 (water/oil 1)	4.90 ± 0.09
System 2 (water/oil 2)	2.96 ± 0.10
System 3 (water/oil 3)	0.58 ± 0.10

Note that System 1 and System 2 are denoted, respectively, as Emulsion 1 and Emulsion 2 after emulsification.

2.1 EXPERIMENTAL BENCH

The experimental bench is schematized in Fig. 1. It is defined by two sets of elements: the first set consists of an IKA EUROSTAR 200 control P4 mixer, to which a cylindrical steel rotor is attached through a mandrel; the second set of the experimental bench is composed of a heavy metal base and a cylindrical acrylic reservoir (stator). These two elements are connected and centered by a plastic cover. The bottom surface of the reservoir is conical ($\alpha = 10^\circ$) and has a perforation in the center, connected to a globe valve that is used to remove the free water phase. The two main sets of the experimental bench must be positioned so that the bottom surface of the cylindrical geometry is at a height $h = 5$ mm above the bottom surface of the reservoir. Also, the geometry and the reservoir must be concentric. To guarantee this condition, we use two homemade accessories. The purpose of the first one is to eliminate angular misalignments, which guarantees the verticality of the cylinder. The second prevents eccentricity.

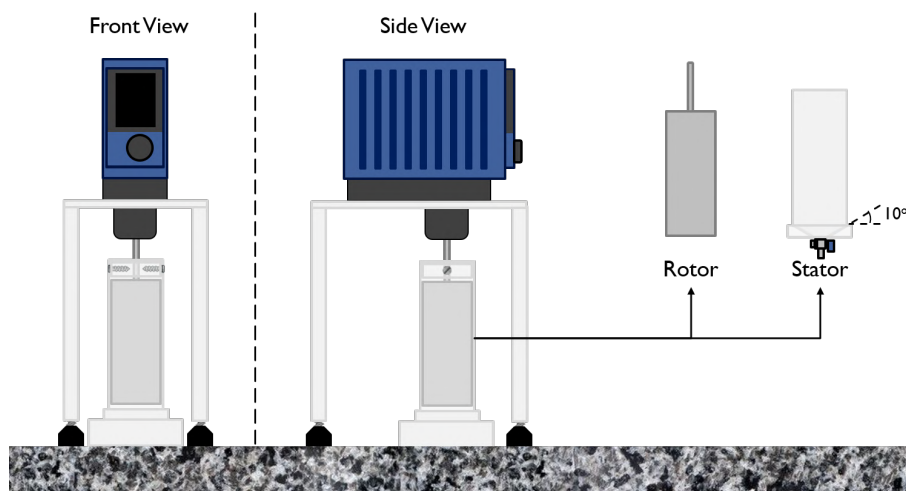


Figure 1. Schematic representation of the experimental bench

We present two flow geometries in this work, namely, Couette and Settling Zones. The former (Fig. 2a)) is a small gap concentric cylinder geometry, in which the confinement ratio of the drops between the rotor and the reservoir is constant. Meanwhile, the latter (Fig. 2b)) presents a variation between zones of greater (coalescence zone) and smaller (settling

zone) confinement of the drops. Note that the gap of the Couette geometry is equal to the average between the gaps of the coalescence and settling zones.

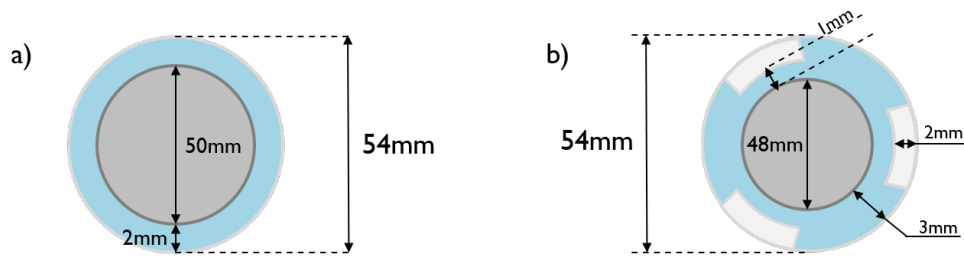


Figure 2. Dimensions of the Couette and Settling Zones flow geometries

2.2 EMULSIFICATION

First, a glass beaker with dimensions $h = 160\text{mm}$ and $D = 44\text{mm}$, designed for this experiment, is placed on a Gehaka semi-analytical BG4400 scale. The balance is tared, and the oil phase is weighed. Afterwards, the balance is tared again, and the surfactant is weighed. These two fluids are homogenized on a magnetic stir plate with the aid of a magnetic bar. After the homogenization, the weighing of the aqueous phase is carried out and the emulsification process begins. The emulsification step takes place in the previously mentioned beaker with the use of an IKA EUROSTAR 200 control P4 mixer along with a custom-made mixing paddle (see Fig. 3). The beaker has two baffles, positioned at 120° from each other. The mixing paddle is positioned vertically, offset and equally distant from each baffle so that mixing is optimized. The mixing protocol consists of three subsequent steps i) 400RPM for 4 minutes ii) 700RPM for 3 minutes iii) 1000RPM for 4 minutes.

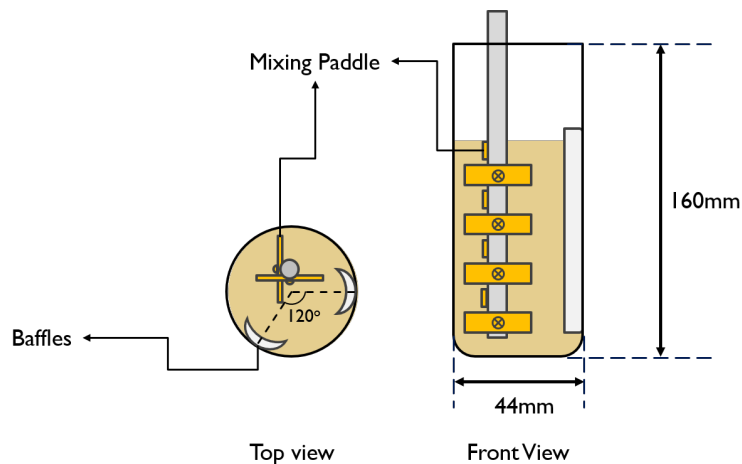


Figure 3. Schematic representation of the glass beaker and mixing paddle

2.3 DROPLET SIZE DISTRIBUTION

After the emulsification, the droplet size distribution of the sample is measured. Samples are discarded if their average droplet diameter greatly differs from the other samples. The droplet size distribution after shearing is not measured because the larger droplets have already separated from the bulk of the emulsion. Therefore, this measure would lead to deceptive results.

A Nikon Eclipse LV100pol optical microscope coupled with a digital camera was used to take photographs, using a 50x objective lens. To guarantee good representative data, 30 photos were taken for each sample. Figure 4(a) shows an example of a photo taken from one of our samples. An algorithm was developed in MatLab to process the photos and measure the size of a droplet. The algorithm takes images as input and converts them to an RGB vector using the function `imread`. Subsequently, the function `imfindcircles` reads the RGB vector and finds circles using name-value pairs to control the Circular Hough Transform (see Fig. 4(b)). A searching algorithm is used to remove the duplicate droplets (see Fig. 4(c)). Finally, the function `bar` takes the vector of diameters, builds a histogram, and fits the probability distribution function to parametric distribution "Kernel" (see Fig. 4(d)) (Marin, 2020). Then, the average droplet diameter is measured.

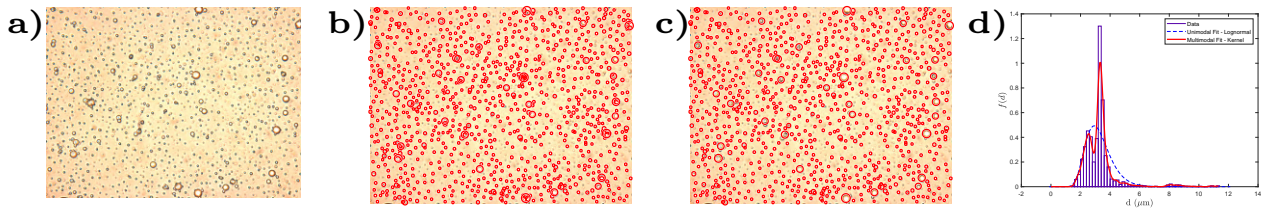


Figure 4. Step by step of the image treatment. (a) Original image, (b) image with all circles, (c) circles without duplicates, and (d) $f(d_p)$

2.4 PHASE SEPARATION EXPERIMENTS

Finally, the sample is taken to the cylindrical reservoir. The samples may remain at rest or be sheared. Shear rate may range from $\gamma = 5$ (1/s) to $\gamma = 20$ (1/s), and the shearing time may be 2h or 4h. These samples remain in the cylindrical reservoir until the end of the observation time. All samples are observed at the end of 24 hours. Once this time has been reached, the free water phase of the emulsions that remained in the reservoir is removed through the globe valve to a certified measuring cylinder in which the volume of the free phase is measured. The phase separation efficiency is given by Eq. 1.

$$\epsilon = \frac{V_{freeWater}}{V_{totalWater}}, \quad (1)$$

3. RESULTS

3.1 DROPLET SIZE DISTRIBUTION

The emulsification protocol guarantees a good agreement between the different samples used in our experiments. The average mean diameter obtained from the droplet size distribution of the 180 samples analyzed in this paper is $d_m = 29.29 \pm 6.06 \mu\text{m}$. Therefore, the average confinement ratio, which is given by the ratio between the average diameter of the sample and the flow gap, is 0.018 for the Couette apparatus. For the Settling Zones apparatus, the average confinement ratio is 0.035 in the coalescence zones and 0.012 in the sedimentation zones.

3.2 PHASE SEPARATION EFFICIENCY

The results are plotted in stacked bar graphs that show the phase separation efficiency in a visually similar manner to the observation of the sample in the experimental setup (Fig. 5a)). Initially, we performed experiments on the Couette geometry with Emulsion 1. The results obtained served as a conceptual proof of the destabilization of the emulsion due to flow-induced coalescence, as seen in Fig. 5b). The phase separation of the emulsion at rest in a separatory funnel was also assessed.

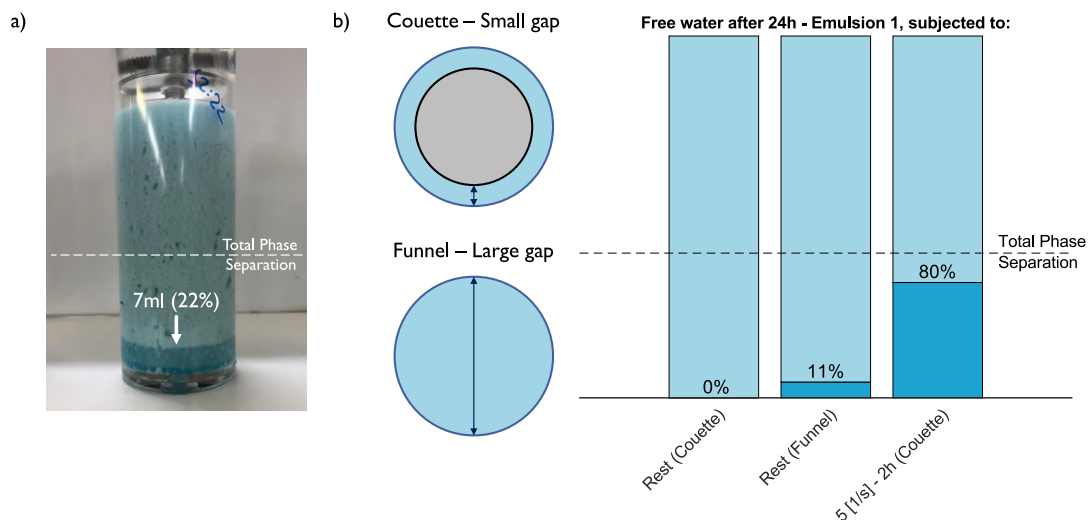


Figure 5. a) Visualization of the phase separation in the apparatus, b) phase separation efficiency for Emulsion 1 at rest at the Couette apparatus and at a separatory funnel - as well as sheared at the Couette apparatus at $\dot{\gamma} = 5$ (1/s) for 2h.

When we compare emulsions at rest, the process efficiency is greater in the separatory funnel than in the Couette geometry. However, the efficiency for emulsions sheared at $\dot{\gamma} = 5$ (1/s) for 2h in the Couette geometry is much higher than the one of the emulsions at rest in both cases. This result shows that flow-induced coalescence increases the phase separation efficiency. On the other hand, it also suggests that the small confinement ratio hinders the sedimentation of the larger droplets due to wall friction since these droplets and their clusters may be of the same magnitude of the gap.

Thus, we designed the previously mentioned Settling Zones apparatus, in which there is a variation between zones of greater and smaller confinement of droplets. The former induces coalescence while the latter allows large droplets to settle. Figure 6 compares the phase separation efficiency of the Couette and the Settling Zones flow geometries for samples at rest and sheared at $\dot{\gamma} = 10$ (1/s) for 1h and 2h. The Settling Zones flow geometry is more efficient than the Couette flow geometry, reaching an efficiency of 73% when the sample is subjected to 2h of shear.

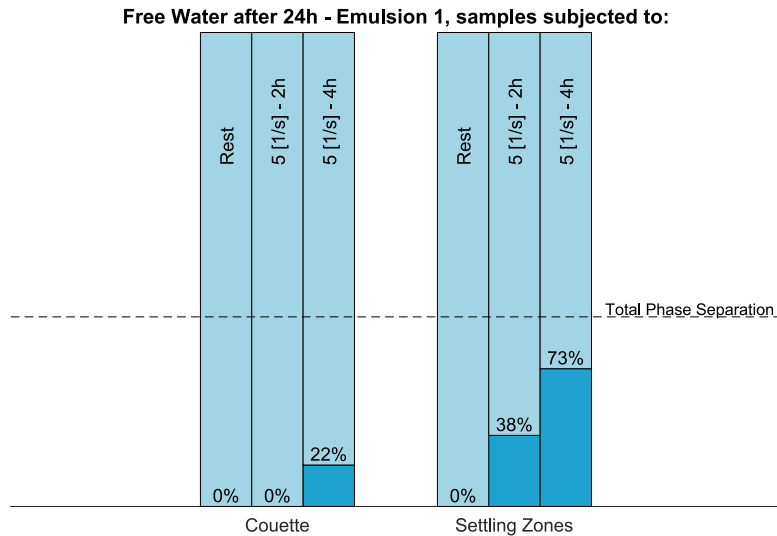


Figure 6. The phase separation efficiency of the Couette vs. the Settling Zones flow geometries

Using the Settling Zones apparatus, we measured the phase separation efficiency for both Emulsion 1, 2 and 3 for a wide range of shear rates. The emulsions were sheared for 4h, and the free water was measured 24h after the beginning of the experiment. The results show that there is an optimal shear at the rate of $\dot{\gamma} = 10$ (1/s) for Emulsion 2 and 3. However, the optimal shear rate for Emulsion 1 is $\dot{\gamma} = 5$ (1/s). The increase of shear rate above this optimal rate leads to droplet breakup - which increases the emulsion stability and decreases the phase separation efficiency. Furthermore, the results show that Emulsion 3 is more stable than Emulsion 2 in general - and both are more stable than Emulsion 1. As expected, this suggests a positive correlation between stability and surfactant concentration (see Table 1), as well as a negative correlation between stability and interfacial tension (see Table 1). Nonetheless, the phase separation efficiency at the optimal shear is virtually the same for Emulsion 2 (72%) and Emulsion 3 (73%).

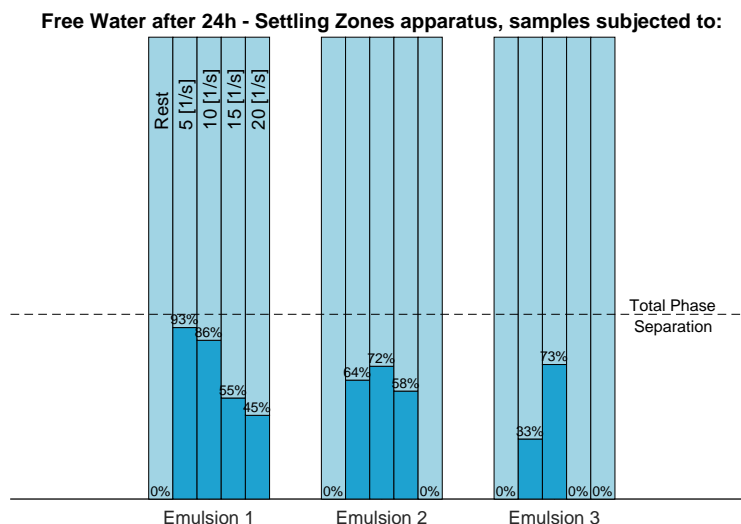


Figure 7. The phase separation efficiency for Emulsions 1, 2 and 3 at various shear rates

4. CONCLUSION

The effect of shearing in the phase separation efficiency is investigated systematically. Flow-induced coalescence is widely reported in the literature, and the results show that this phenomenon may increase the phase separation efficiency of emulsions. However, high shear rates may cause droplet breakup, and, thus, increase the stability of the system. Moreover, sedimentation is also required for phase separation. Even though confined flow may favor coalescence, it also hinders the sedimentation of the larger droplets due to wall friction since these droplets and their clusters may be of the same magnitude of the gap. The use of a flow geometry with alternation between zones of greater and smaller confinement of droplets optimizes the trade-off between flow-induced coalescence and sedimentation. This concept may be extended to design a novel equipment for oil processing plants. The use of droplet deformation renders this technique more efficient than gravity settling alone.

Initially, we obtained a conceptual proof of the destabilization of the emulsion due to flow-induced coalescence, by comparing systems at rest and sheared, in the Couette geometry. Furthermore, we compared the phase separation efficiency on both the Couette and Settling Zones geometry. The latter presented higher efficiency due to the variation between zones of greater and smaller confinement of the drops, which allows for both coalescence and sedimentation to occur. Finally, we assessed the efficiency of the phase separation process of three systems with different surfactant concentrations and interfacial tensions in the Settling Zones geometry. The results suggest a positive correlation between stability and surfactant concentration, as well as a negative correlation between stability and interfacial tension. All systems presented an optimal shear-rate above which droplet-breakup occurs, thus increasing the emulsion stability and decreasing the phase separation efficiency.

The phase separation efficiency may be further optimized by experimenting with geometrical parameters such as the confinement ratio and the number and, consequently, length of the coalescence and settling zones. Moreover, water wash could also be implemented. In this case, the sheared droplets would come into contact with an excess phase and thus be removed from the continuous phase. Water wash is a well-known method to increase the phase separation efficiency, and it would be further favored by the deformation of droplets due to the increase in the contact area between the droplets and the excess phase.

5. ACKNOWLEDGEMENTS

The authors thank Petrobras S. A. (2017/00426-9), ANP(PRH-01.19.0248.00), CNPq(307976/2018-1), CAPES (PROEX 625/2018), and FAPERJ(E-26/202.834/2017) for the financial support to the Rheology Group at PUC-Rio.

6. REFERENCES

The list of references must be introduced as a new section, located at the end of the manuscript. The first line of each reference must be aligned at left. All the other lines must be indented by 0.5 cm from the left margin. All references included in the reference list must have been mentioned in the text.

References must be listed in alphabetical order, according to the last name of the first author. See the following examples:

- Aleem, W. and Mellon, N., 2012. "Population balance model for batch gravity separation of crude oil and water emulsions. part ii: Comparison to experimental crude oil separation data". *Journal of Dispersion Science and Technology*, Vol. 33, pp. 591–598.
- Aleem, W. and Mellon, N., 2018. "Model for the prediction of separation profile of oil-in-water emulsion". *Journal of Dispersion Science and Technology*, Vol. 39, pp. 8–17.
- Allan, R. and Mason, S., 1962. "Particle behaviour in shear and electric fields i. deformation and burst of fluid drops". *Proceedings of the Royal Society of London. Series A. Mathematical and Physical Sciences*, Vol. 267, pp. 45–61.
- Barai, N. and Mandal, N., 2019. "Breakup versus coalescence of closely packed fluid drops in simple shear flows". *International Journal of Multiphase Flow*, Vol. 111, pp. 1–15.
- Chen, D., Cardinaels, R. and Moldenaers, P., 2009. "Effect of confinement on droplet coalescence in shear flow". *Langmuir*, Vol. 25, pp. 12885–12893.
- De Bruyn, P., Cardinaels, R. and Moldenaers, P., 2013. "The effect of geometrical confinement on coalescence efficiency of droplet pairs in shear flow". *Journal of colloid and interface science*, Vol. 409, pp. 183–192.
- Dicharry, C., Arla, D., Sinquin, A., Graciaa, A. and Bouriat, P., 2006. "Stability of water/crude oil emulsions based on interfacial dilatational rheology". *Journal of colloid and interface science*, Vol. 297, pp. 785–791.
- Eow, J.S. and Ghadiri, M., 2003. "Motion, deformation and break-up of aqueous drops in oils under high electric field strengths". *Chemical Engineering and Processing: Process Intensification*, Vol. 42, pp. 259–272.
- Fan, Y., Simon, S. and Sjöblom, J., 2010. "Interfacial shear rheology of asphaltenes at oil–water interface and its relation to emulsion stability: Influence of concentration, solvent aromaticity and nonionic surfactant". *Colloids and Surfaces*

A: *Physicochemical and Engineering Aspects*, Vol. 366, pp. 120–128.

- Fischer, P. and Erni, P., 2007. “Emulsion drops in external flow fields—the role of liquid interfaces”. *Current Opinion in Colloid & Interface Science*, Vol. 12, pp. 196–205.
- Fortuny, M., Oliveira, C.B., Melo, R.L., Nele, M., Coutinho, R.C. and Santos, A.F., 2007. “Effect of salinity, temperature, water content, and ph on the microwave demulsification of crude oil emulsions”. *Energy Fuels*, Vol. 21, No. 3, pp. 1358–1364.
- Gouseti, O., Watson, N. and Pacek, A., 2020. “A rheo-optic study of liquid/liquid systems with varying phases, volume fractions and viscosity ratios”. *Food and Bioproducts Processing*, Vol. 123, pp. 251–261.
- He, X., Wang, S.L., Yang, Y.R., Wang, X.D. and Chen, J.Q., 2020. “Electro-coalescence of two charged droplets under pulsed direct current electric fields with various waveforms: A molecular dynamics study”. *Journal of Molecular Liquids*, Vol. 312, p. 113429.
- Kamp, J., Villwock, J. and Kraume, M., 2017. “Drop coalescence in technical liquid/liquid applications”. *Reviews in Chemical Engineering*, Vol. 33, pp. 1–47.
- Karyappa, R.B., Naik, A.V. and Thaokar, R.M., 2016. “Electroemulsification in a uniform electric field”. *Langmuir*, Vol. 32, pp. 46–54.
- Korobko, A., Van Den Ende, D., Agterof, W. and Mellema, J., 2005. “Coalescence in semiconcentrated emulsions in simple shear flow”. *The Journal of chemical physics*, Vol. 123, p. 204908.
- Leal, L., 2004. “Flow induced coalescence of drops in a viscous fluid”. *Physics of fluids*, Vol. 16, pp. 1833–1851.
- Li, N., Sun, Z., Liu, W., Wei, L., Li, B., Qi, Z. and Wang, Z., 2021. “Effect of electric field strength on deformation and breakup behaviors of droplet in oil phase: A molecular dynamics study”. *Journal of Molecular Liquids*, Vol. 333, p. 115995.
- Marin, E., 2020. *Linking the rheology of W/O crude emulsions with the droplet aggregation process*. Ph.D. thesis, Mechanical Engineering, Pontifícia Universidad de Rio de Janeiro, Rio de Janeiro, Brazil.
- Mazumdar, M., Jammoria, A.S. and Roy, S., 2017. “Effective rates of coalescence in oil–water dispersions under constant shear”. *Chemical Engineering Science*, Vol. 157, pp. 255–263.
- Pauchard, V., Rane, J.P., Zarkar, S., Couzis, A. and Banerjee, S., 2014. “Long-term adsorption kinetics of asphaltenes at the oil–water interface: A random sequential adsorption perspective”. *Langmuir*, Vol. 28, pp. 8381–8390.
- Rane, J.P., Zarkar, S., Pauchard, V., Mullins, O.C., Christie, D., Andrews, A.B., Pomerantz, A.E. and Banerjee, S., 2015. “Applicability of the langmuir equation of state for asphaltene adsorption at the oil–water interface: Coal-derived, petroleum, and synthetic asphaltenes”. *Energy & Fuels*, Vol. 29, pp. 3584–3590.
- Samaniuk, J.R., Hermans, E., Verwijlen, T., Pauchard, V. and Vermant, J., 2015. “Soft-glassy rheology of asphaltenes at liquid interfaces”. *Journal of Dispersion Science and Technology*, Vol. 36, pp. 1444–1451.
- Spiecker, P.M. and Kilpatrick, P.K., 2004. “Interfacial rheology of petroleum asphaltenes at the oil- water interface”. *Langmuir*, Vol. 20, pp. 4022–4032.
- Vu, T.V., 2019. “Parametric study of the collision modes of compound droplets in simple shear flow”. *International Journal of Heat and Fluid Flow*, Vol. 79, p. 108470.
- Yang, X., Verruto, V.J. and Kilpatrick, P.K., 2007. “Dynamic asphaltene-resin exchange at the oil/water interface: Time-dependent w/o emulsion stability for asphaltene/resin model oils”. *Energy & fuels*, Vol. 21, pp. 1343–1349.
- Zarkar, S., Pauchard, V., Farooq, U., Couzis, A. and Banerjee, S., 2015. “Interfacial properties of asphaltenes at toluene–water interfaces”. *Langmuir*, Vol. 31, pp. 4878–4886.

7. RESPONSIBILITY NOTICE

The authors are solely responsible for the printed material included in this paper.